SPACE WEATHER, VOL. 5, S04002, doi:10.1029/2006SW000286, 2007

East-west asymmetry in coronal mass ejection geoeffectiveness

G. Siscoe,[1] P. J. MacNeice,[2] and D. Odstrcil[3]

Received 26 September 2006; revised 17 November 2006; accepted 20 November 2006; published 3 April 2007.

[1] This paper extends the domain of applicability of the Gosling-McComas space weather forecast rule that applies to the postshock sheaths of fast coronal mass ejections at Earth (ICMEs). The rule is based on the draping of the sheath magnetic field around the ICME body. The original treatment considered only the radial-from-the-Sun component of the preshock interplanetary magnetic field (IMF), which implied that the domain of applicability of the rule was the entire sheath region ahead of the leading face of the ICME. We show here that because of the generally prevailing Parker spiral orientation of the IMF, the domain of applicability of the rule is instead generally strongly shifted to the east side of the ICME sheath. We suggest that the eastward shift of the domain of applicability of the rule accounts for an observed greater geoeffectiveness of west hemisphere CMEs compared with east hemisphere CMEs. The approach used here to demonstrate the eastward shift of the region of potential ICME sheath geoeffectiveness, and thus to increase the accuracy of the forecast rule, is to present intensity contours of the geoeffective draping component of the IMF as computed by global MHD simulations. Since the shift depends only on a spiral magnetic field and a blunt object to drape it around, we demonstrate the generality of the principle on which the rule is based by treating both the case of the ICME and the case of Earth's magnetosphere.

Citation: Siscoe, G., P. J. MacNeice, and D. Odstrcil (2007), East-west asymmetry in coronal mass ejection geoeffectiveness, *Space Weather*, *5*, S04002, doi:10.1029/2006SW000286.

1. Introduction

[2] *Gosling and McComas* [1987] suggested that draping of the interplanetary magnetic field (IMF) around an oncoming fast coronal mass ejection at Earth (ICME) is a mechanism for generating a geoeffective, southward IMF for a duration long enough to induce a magnetic storm and thus to account for the known geoeffectiveness of ICME sheaths [*Gosling et al.*, 1991]. The original Gosling and McComas version of the mechanism focused on the radial component of the IMF since it is this component that must be deflected north or south to let the ICME pass through. According to their model, whether the resulting draping produces a nongeoeffective northward or geoeffective southward IMF at Earth depends on the radial orientation of the IMF (toward or away for the Sun) and on whether the nose of the ICME passes to the north or south of Earth. The corresponding forecast rule can be written as: ''geoeffective events occur when the IMF points away from (toward) the Sun and the ICME passes southward (northward) of Earth.'' Both the toward-away polarity of the IMF and the north-south passage of the ICME can be forecast at the time of the CME on the Sun. Thus the Gosling-McComas forecast rule could have genuine usefulness in the forecast community. *McComas et al.* [1989] tested the model's predictions of ICME-induced north-south IMF orientations and found agreement in 13 of 17 events. This paper suggests that modifying the rule to take account of an east-west asymmetry in its applicability should improve its robustness and accuracy.

[3] First we need to make clear what is meant by east and west in the solar context. These directions refer to the astronomical convention which projects the terrestrial sense of east and west onto the celestial sphere. The astronomical convention is also used in solar physics. For a northern hemisphere observer, it means that when looking at the Sun east is to the left and west is to the right. (This convention has the confusing consequence that the Sun rotates from east to west.)

[4] The mentioned modification concerns an eastward shift in the ICME sheath of the region of applicability of

[1]Center for Space Physics, Boston University, Boston, Massachusetts, USA.
[2]Community Coordinated Modeling Center, Goddard Space Flight Center, Greenbelt, Maryland, USA.
[3]Space Environment Center, NOAA, Boulder, Colorado, USA.

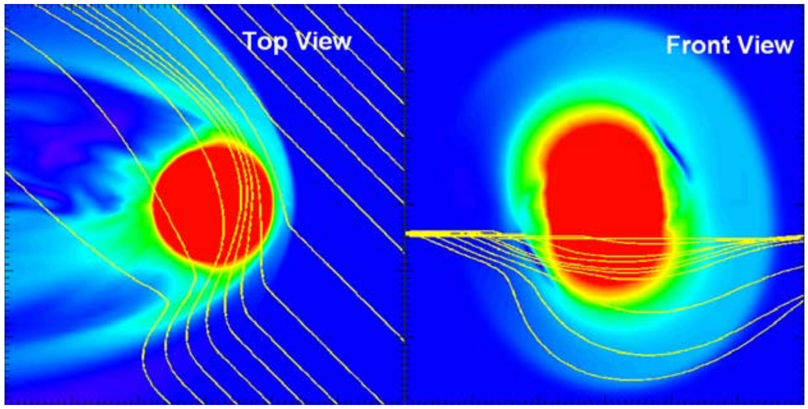

Figure 1. Draping of Parker spiral field lines in Earth's magnetosheath around the magnetosphere showing asymmetric field strength and out-of-plane draping of field lines that lie south of the equatorial plane in the solar wind.

the rule. This suggestion is motivated by the reports by *Wang et al.* [2002], *Zhang et al.* [2003], and *Zhao et al.* [2006] that west hemisphere CMEs are more geoeffective than east hemisphere CMEs. Centrally located CMEs are, of course, most geoeffective, but away from the central region, west hemisphere CMEs apparently dominate. For example, in the Wang et al. study of 59 geoeffective CMEs, none were located eastward of 39°E whereas 8 were located westward of 39°W. Similarly, Zhang et al. found that of 21 CMEs associated with major magnetic storms 1 was located east of 30°E whereas 6 were located west of 30°W. The Zhao study found that ''Most severe geomagnetic storms ($Dst_{\min} < -100$ nT) are usually caused by flare-associated shocks originating from western hemisphere or middle regions near central meridian''.

[5] What could cause such an asymmetry? It is not that there are more Earth-impacting CMEs from the western hemisphere, since *Cane et al.* [2000] and *Wang et al.* [2002] have shown that these are uniformly distributed in longitude. Zhang et al. point instead to the east-west asymmetry that the spiral interplanetary magnetic field imposes on the situation. As a mechanism, they suggest that shock waves of western CMEs might have a better chance of reaching Earth by following the IMF. Zhao et al. also suggest that the shocks associated with west hemisphere flares are more likely to reach Earth.

[6] This paper adopts the part of the *Zhang et al.* [2003] and *Zhao et al.* [2006] suggestion that attributes the cause of the observed east-west asymmetry in CME geoeffectiveness to the spiral geometry of the IMF. However, instead of a mechanism based on an asymmetry in shock propagation, it identifies a mechanism based on an east-west asymmetry in ICME sheaths, since it seems likely than any storm caused by a CME with a longitude of 40° or greater is a pure sheath-induced storm. The mechanism we propose is the same as that of Gosling and McComas modified to take account of the Parker spiral magnetic field. The eastward shift in the location of the application of the Gosling-McComas forecast rule is intuitively obvious if one thinks of the IMF as being a vacuum field and the ICME body as being a perfect conductor. Then the location of maximum draping coincides with the null point where the IMF splays out on contact with the ICME surface. This would be at the nose of the ICME if the IMF were strictly radial (the Gosling-McComas case), but well to the east of the nose for a 45° Parker spiral IMF.

[7] Of course, the IMF does not exist in a vacuum, and so here we treat the problem in an MHD context. The main result is that the vacuum conclusion is upheld. The approach is to use global MHD simulations of the Parker spiral IMF draping around Earth's magnetosphere and around an ICME. That the eastward shift in maximum out-of-plane draping occurs in both cases (in the Earth's case it is a dawnward shift) shows that the effect is generic. The use of an MHD simulation of draping around Earth's magnetosphere to discuss draping around ICMEs has been validated by *Kaymaz and Siscoe* [2006] who showed that observed in-plane draping in ICME sheaths matches well the computed draping for the terrestrial case even in the flank where draping distortion maximizes. Here we use both the terrestrial simulation and an ICME simulation to look at the draping behind the Gosling-McComas forecast rule.

2. Asymmetric Out-of-Plane Draping Around Earth's Magnetosphere

[8] Figure 1 shows top and front views of draping of a Parker spiral field in the magnetosheath around Earth's magnetosphere as computed by the ISM global magnetospheric MHD code [*White et al.*, 2001]. The colors, which indicate field strength, serve to define the body that is plowing through the IMF and forcing it to drape around the body as it passes. In the solar wind upstream from the bow shock the field lines lie in a plane 0.5 body lengths south of the equatorial plane, where ''body length'' refers to the radius of curvature of the body at the nose. The field

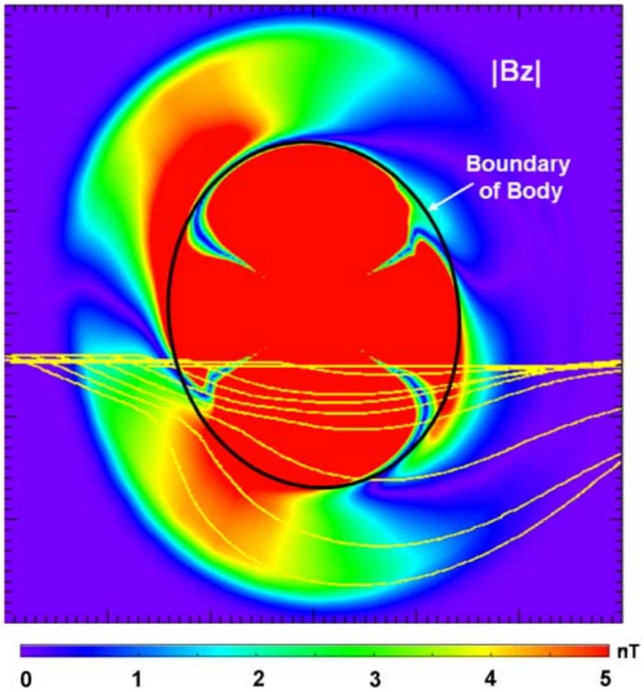

Figure 2. Magnitude of the out-of-plane magnetic field component in Earth's magnetosheath in a plane about one body length downwind from the nose of the body. The view is from the Sun. The boundary of the body is roughly indicated by the ellipse. The field inside the ellipse belongs to the body and is not relevant to the present discussion.

lines in the top view (left frame) pass underneath the body and are seen through it. The field lines in the front view show the claimed dawn-dusk asymmetry in out-of-plane draping, by which we mean draping that produces a component of the IMF that is out of the plane of the preshock Parker spiral.

[9] The solar wind parameters used to initialize the MHD run that produced the images in Figure 1 were given typical values: V = 350 km/s, n = 5 protons/cm^3, T = 20 eV, B = 5 nT, field lines lay in planes parallel to the equatorial plane, were oriented away from the Sun, and were inclined 45° with respect to the radial-from-Sun direction. The geomagnetic dipole was oriented perpendicular to the solar wind flow direction. The factor of two stronger field at the pole of a dipole compared to the equator causes an ellipticity in the shape of the field strength contours in the front view. This aspect of Figure 1 is irrelevant to the case of ICMEs, which appear to have a more nearly circular cross section [*Schwenn et al.*, 2005]. Another irrelevant aspect is the presence in the front view of two slivers of dark blue (very weak field) in the upper right and lower left of the boundary between the body and its sheath. These are expressions of the so-called magnetospheric sash [*White et al.*, 1998] that results from antiparallel alignment of the internal and external magnetic fields at these locations for the given IMF orientation. Such antiparallel alignments might also exist at the boundary between ICME bodies and their sheaths, but they play no direct role in the draping phenomenon under consideration here.

[10] Figure 1 shows that the magnetic field in the magnetosheath is weaker on the dawn side than on the dusk side. This asymmetry arises because the shock wave on dawn side is a parallel shock for which the jump in field strength is minimal, whereas the dusk side has a perpendicular shock, where it is maximal. This predicted systematic dawn-dusk asymmetry in magnetosheath field strength has in fact been observed [*White et al.*, 1998]. One expects a similar asymmetry in ICME sheaths for the same reason: other things being equal the field should be weaker in the east flank of an ICME sheath than in the west flank. Such an asymmetry would tend to make east hemisphere CMEs more geoeffective than west hemisphere CMEs, contrary to observations. However the difference in field strength is more than compensated for by the difference in "draping strength" as can be seen in Figure 2.

[11] Figure 2 shows the magnitude of the north-south component (z component) of the magnetic field in a plane about one body length behind the nose of the body. (Figure 2 shows $|B_z|$ instead of B_z since the point of Figure 2 is to demonstrate the dawn-dusk asymmetry in the magnitude of out-of-plane component of B. The sign of B_z is important in the case of ICMEs where it is specified as part of the forecast rule.) The same, marked dawn-dusk asymmetry pattern persists right up to the nose of the body. Of course closer to the nose the pattern is smaller and weaker, nonetheless, within the volume of most of the magnetosheath's dawn flank, the magnitude of the out-of-plane field component is comparable to or larger than the ambient IMF field strength (5 nT in this case), whereas within the corresponding volume of the dusk flank it is near zero almost everywhere. In the ICME context where the dawn flank corresponds to the east flank, whether the z component at a particular place is positive (and, so, not geoeffective) or negative (and, so, geoeffective) depends on the orientation of the ambient IMF and on whether the chosen place is north or south (approximately) of the nose of the ICME. These are the same prediction criteria used by *McComas et al.* [1989] for the front of an ICME sheath only now they apply to the east flank of the sheath.

[12] We note that in Figure 2 the north-south asymmetry in the pattern of $|B_z|$ in the magnetosheath has to do with the geometry of magnetic reconnection at Earth's magnetopause for the 90° IMF clock angle case. Magnetic reconnection changes the boundary conditions at the inner boundary of the magnetosheath and so affects the flow and field configuration within the magnetosheath. A corresponding asymmetry might arise also in ICME sheaths if magnetic reconnection occurs between the IMF and ICME magnetic field, but it would most likely vary from event to event in a way that would be difficult to predict, depending on the orientation of the magnetic field

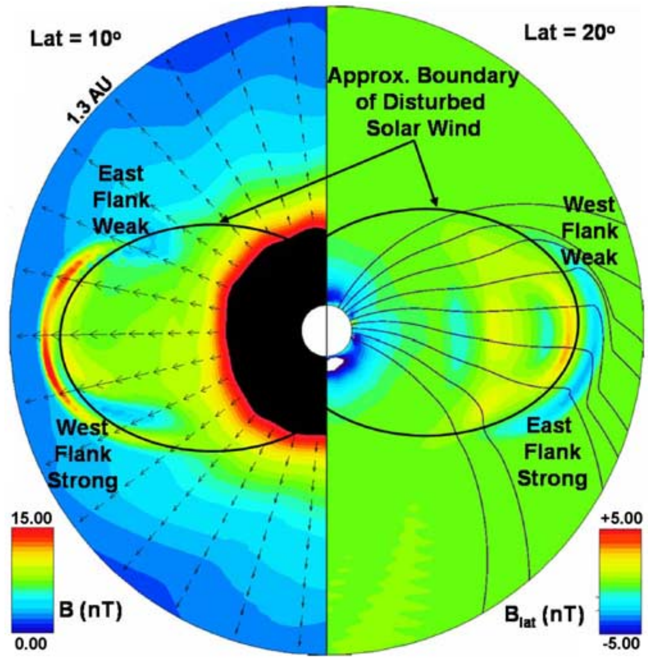

Figure 3. (left) Total magnetic field strength in a constant 10° latitude surface (which approximately cuts the center of the ICME) and (right) out-of-plane magnetic field strength in a constant 20° latitude surface (which is approximately where the east-west asymmetry maximizes) in the sheath of an equatorially launched ICME. The vectors in the left half of the figure show velocity, the maximum value of which, at the leading edge of the ICME, is 1060 km/s. The right half of the figure was rotated 180° from its original orientation to make one circular figure instead of two side-by-side figures like the one on the left. The ellipses approximately outline the forward boundary of the ICME body as identified by a distinctive entropy ridge marking the ICME sheath. The field inside the ellipse belongs to the body and is not relevant to the present discussion.

within the ICME body. For the present discussion it represents a complication but not a barrier to implementation.

3. Asymmetric Out-of-Plane Draping Around an ICME

[13] Figure 3 shows IMF intensity contours and field line draping around an ICME sheath as computed by the cone model [*Zhao et al.*, 2002] as linked to a global heliospheric MHD code called ENLIL [*Odstrcil et al.*, 2004] as implemented at the Community Coordinated Modeling Center (http://ccmc.gsfc.nasa.gov, run number 080906_SH_1). The CME was launched on the equator during a stretch of unipolar magnetic field during Carrington rotation 1909 when the heliospheric current sheet lay nearly in the equatorial plane so that there were no significant corotating interaction regions that might complicate the interpretation.

[14] The computation is generated by running two coupled models, ENLIL and the Wang-Sheeley-Arge model (WSA). The WSA [*Arge and Pizzo*, 2000] model combines a potential source surface solution for the coronal magnetic field between the solar surface and 2.5 solar radii, with a pseudopotential current sheet model between 2.5 and 21.5 solar radii. It uses a photospheric synoptic magnetogram to set the radial magnetic flux at the solar surface, in this case a Kitt Peak magnetogram for Carrington Rotation 1909.

[15] The ENLIL code [*Toth and Odstrcil*, 1996] solves the 3D MHD equations using a spherical coordinate grid. In this case the grid extended from 21.5 and 431 solar radii (2 AU), and between latitudes 30° to 150°. The WSA magnetic field solution at 21.5 solar radii is used to set the inner boundary condition of the magnetic field at the ENLIL inner boundary. Otherwise, for this calculation the inner boundary density was set to 300 cm^{-3}, the plasma temperature to 8×10^5 K, and the flow speed to 625 km/s. ENLIL then integrated for a period of 12 days to allow the solution to relax to equilibrium, consistent with the field and plasma conditions specified at the rotating inner boundary at 21.5 solar radii. At the end of this equilibrium phase, corresponding to the beginning of CR1909, a cone model CME was launched from the solar equator (latitude 90°) at longitude 360 (equivalent to a start time of 0800 hours on 5 May 1996). It had an initial velocity of 2000 km/s, a density which was 4 times the density of the background fast solar wind, and a temperature which was the same as that of the fast solar wind. The cloud had a spherical initial profile, with a radius of 25°. The frames shown in Figure 3 show the ICME when its nose had just passed the orbit of Earth.

[16] The left side of Figure 3 gives field strength contours in the 10° latitude surface, which is approximately the latitudinal center of the ICME at 1 AU (as seen in Figure 4). Although the boundary between the ICME body and the ICME sheath is not explicitly calculated by the code, it can be approximately identified by a marked entropy ridge in the ICME sheath caused by the ICME shock on the outside and the low-entropy ICME plasma on the inside. The leading front of the boundary thus identified is indicated by ellipses. (The trailing edge is not meant to be so indicated, since an ellipse does not fit the entire boundary.)

[17] Figure 3 shows that the same shock-induced, east-west asymmetry in field strength occurs in ICME sheaths as in Earth's magnetosheath as seen in Figure 1. The field is weaker on the side with the parallel shock (the east flank) and stronger on the side with the perpendicular shock (the west flank). That the IMF is weaker on the east flank of the ICME sheath and that this asymmetry results from the properties of the ICME bow shock interacting with the spiral magnetic field argues against the previously mentioned shock mechanism suggested by *Zhang et al.* [2003] and *Zhao et al.* [2006].

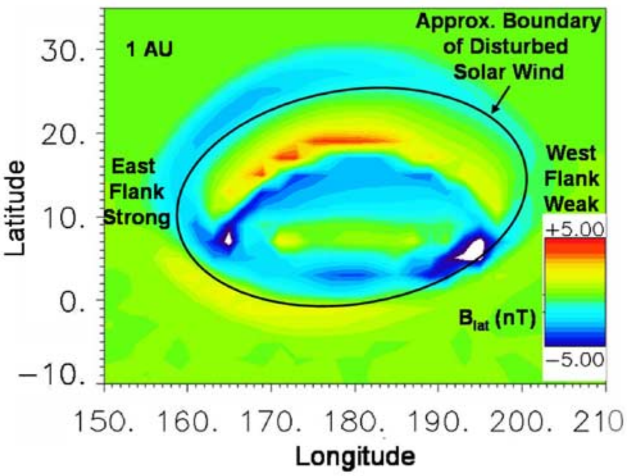

Figure 4. Strength of out-of-plane magnetic field component (B_{lat}) in a constant radius surface ($r = 1$ AU). The view is toward the Sun. The ellipse approximately outlines the boundary of the ICME body as identified by a distinctive entropy ridge marking the ICME sheath. The field inside the ellipse belongs to the body and is not relevant to the present discussion. The eastward shift of the region of strongest out-of-plane field in the sheath is evident.

[18] By contrast the right side of Figure 3 shows that the out-of-plane component (B_{lat}) is stronger on the east flank where the IMF intersects the body most perpendicularly, as in the terrestrial case. The out-of-plane field strength maximizes at about 5 nT, which is comparable to the ambient value upstream from the shock. Thus unlike the shock mechanism, the Gosling-McComas draping mechanism has the correct east-west asymmetry to account for the observed asymmetry in CME geoeffectiveness.

[19] Figure 4 shows the out-of-plane component in an r = constant surface ($r = 1$ AU). This is the heliospheric counterpart to Figure 2. Even though the CME was launched at the solar equator, the ICME at 1 AU appears to have ''migrated'' northward, but this is not a real northward motion of the ICME. The northward location of the center of the body seen in this $r = 1$ surface results from a distortion of the ICME in the r latitude plane as it propagates into a southward inclined streamer belt. The rest of the southward part of the ICME has not yet reached the $r = 1$ AU surface. (See *Odstrcil and Pizzo* [1999] for an illustration and discussion of such distortion.) Here as in Figure 2 one sees an eastward shift of maximum out-of-plane field that occurs in both northern and southern hemispheres.

[20] If the orientation of the out-of-plane component happens to be southward, it could be quite geoeffective since in the case shown here it is moving at between 700 km/s and 800 km/s. Depending on just where along the flank the Earth happens to be when the ICME passes, the duration of Earth's exposure to this geoeffective field could be between 3 and 6 hours, which is long enough to generate at least a moderate magnetic storm. Of course the single case discussed here only serves to show that out-of-plane draping of the IMF around fast ICMEs can provide a systematic geoeffective magnetic field on the east flanks of ICMEs. It does not explore conditions that would maximize the geoeffectiveness of the proposed mechanism.

4. Summary

[21] The Gosling-McComas rule for forecasting the relative geoeffectiveness of the sheaths of fast ICME has been modified in this paper to take account of the spiral nature of the IMF. The modification significantly shifts the region of application of the rule from the nose of the ICME to its eastward flank. This eastward shift applies to the usual case in which the preshock IMF has the Parker spiral orientation. However, the treatment of the problem given here allows the rule to be tailored for application to any situation in which the orientation of the preshock IMF is known. The general rule becomes: ''shift the center of application of the rule to the point on the ICME body at which the preshock IMF points most directly.'' For standard forecast operations, however, information on the preshock IMF would be obtained from the Wang-Sheeley-Arge model, which predicts only the toward-away polarity of the IMF; thus one must assume Parker spiral geometry in applying the forecast rule. It should be emphasized that the sheaths of fast ICMEs can be very geoeffective. Thus standard application of the Gosling-McComas rule as modified here could add importantly to space weather forecasting services.

[22] **Acknowledgments.** The work at Boston University was supported in part by the National Science Foundation under grant ATM-0220396. Simulation results have been provided by the Community Coordinated Modeling Center at Goddard Space Flight Center through their public Runs on Request system (http://ccmc.gsfc.nasa.gov). The CCMC is a multiagency partnership between NASA, AFMC, AFOSR, AFRL, AFWA, NOAA, NSF, and ONR. The ENLIL-cone model was developed by D. Odstrcil at the Cooperative Institute for Research in Environmental Sciences at the University of Colorado and National Oceanic and Atmospheric Administration under NASA/LWS-TR&T and as part of the CISM project which is funded by the STC Program of the National Science Foundation under agreement ATM-0120950.

References

Arge, C. N., and V. J. Pizzo (2000), Improvement in the prediction of solar wind conditions using near-real time solar magnetic field updates, *J. Geophys. Res.*, *105*, 10,465–10,480.

Cane, H. V., I. G. Richardson, and O. C. St. Cyr (2000), Coronal mass ejections, interplanetary ejecta and geomagnetic storms, *Geophys. Res. Lett.*, *27*, 3591–3594.

Gosling, J. T., and D. J. McComas (1987), Field line draping about fast coronal mass ejecta: A source of strong out-of-the-ecliptic interplanetary magnetic fields, *Geophys. Res. Lett.*, *14*, 355 – 358.

Gosling, J. T., D. J. McComas, J. L. Phillips, and S. J. Bame (1991), Geomagnetic activity associated with Earth passage of interplanetary shock disturbances and coronal mass ejections, *J. Geophys. Res.*, *96*, 7831 – 7839.

Kaymaz, Z., and G. Siscoe (2006), Field-line draping around ICMEs, *Sol. Phys.*, *239*, 437 – 448.

McComas, D. J., J. T. Gosling, S. J. Bame, E. J. Smith, and H. V. Cane (1989), A test of magnetic field draping induced B_z perturbations ahead of fast coronal mass ejecta, *J. Geophys. Res.*, *94*, 1465 – 1471.

Odstrcil, D., and V. J. Pizzo (1999), Distortion of the interplanetary magnetic field by three-dimensional propagation of coronal mass ejections in a structured solar wind, *J. Geophys. Res.*, *104*, 28,225 – 28,240.

Odstrcil, D., P. Riley, and X. P. Zhao (2004), Numerical simulation of the 12 May 1997 interplanetary CME event, *J. Geophys. Res.*, *109*, A02116, doi:10.1029/2003JA010135.

Schwenn, R., A. Dal Lago, E. Huttunen, and W. D. Gonzalez (2005), The associations of coronal mass ejections with their effects near the Earth, *Ann. Geophys.*, *23*, 1033 – 1059.

Toth, G., and D. Odstrcil (1996), Comparison of some flux corrected transport and total variation diminishing numerical schemes for hydrodynamic and magnetohydrodynamic problems, *J. Comput. Phys.*, *128*, 82 – 100.

Wang, Y. M., P. Z. Ye, S. Wang, G. P. Zhou, and J. X. Wang (2002), A statistical study on the geoeffectiveness of Earth-directed coronal mass ejections from March 1997 to December 2000, *J. Geophys. Res.*, *107*(A11), 1340, doi:10.1029/2002JA009244.

White, W. W., G. L. Siscoe, G. M. Erickson, Z. Kaymaz, N. C. Maynard, K. D. Siebert, B. U. Ö. Sonnerup, and D. R. Weimer (1998), The magnetospheric sash and the cross-tail S, *Geophys. Res. Lett.*, *25*, 1605 – 1608.

White, W. W., J. A. Schoendorf, K. D. Siebert, N. C. Maynard, D. R. Weimer, G. L. Wilson, B. U. Ö. Sonnerup, G. L. Siscoe, and G. M. Erickson (2001), MHD simulation of magnetospheric transport at the mesoscale, in *Space Weather, Geophys. Monogr. Ser.*, vol. 125, edited by P. Song, H. J. Singer, and G. L. Siscoe, pp. 229 – 240, AGU, Washington, D. C.

Zhang, J., K. P. Dere, R. A. Howard, and V. Bothmer (2003), Identification of solar sources of major geomagnetic storms between 1996 and 2002, *Astrophys. J.*, *582*, 520 – 533.

Zhao, X. P., S. P. Plunkett, and W. Liu (2002), Determination of geometrical and kinematical properties of halo coronal mass ejections using the cone model, *J. Geophys. Res.*, *107*(A8), 1223, doi:10.1029/2001JA009143.

Zhao, X., X. Feng, and C.-C. Wu (2006), Characteristics of solar flares associated with interplanetary shock or nonshock events at Earth, *J. Geophys. Res.*, *111*, A09103, doi:10.1029/2006JA011784.

P. J. MacNeice, Community Coordinated Modeling Center, Goddard Space Flight Center, Greenbelt, MD 20771, USA.

D. Odstrcil, Space Environment Center, NOAA, Boulder, CO 80303, USA.

G. Siscoe, Center for Space Physics, Boston University, 725 Commonwealth Ave., Boston, MA 02215, USA. (siscoe@bu.edu)